Insights into Hydrogen Atom Adsorption on and the Electrochemical Properties of Nitrogen-Substituted Carbon Materials

Z. H. Zhu,*,† H. Hatori,‡ S. B. Wang,§ and G. Q. Lu†

ARC Centre for Functional Nanomaterials, University of Queensland, Brisbane, 4072, Australia, Energy Technology Research Institute, National Institute of Advanced Industrial Science and Technology (AIST), Tsukuba, Japan, and Department of Chemical Engineering, Curtin University of Technology, Perth, Australia

Received: April 7, 2005; In Final Form: June 24, 2005

The nitrogen substitution in carbon materials is investigated theoretically using the density functional theory method. Our calculations show that nitrogen substitution decreases the hydrogen adsorption energy if hydrogen atoms are adsorbed on both nitrogen atoms and the neighboring carbon atoms. On the contrary, the hydrogen adsorption energy can be increased if hydrogen atoms are adsorbed only on the neighboring carbon atoms. The reason can be explained by the electronic structures analysis of N-substituted graphene sheets. Nitrogen substitution reduces the π electron conjugation and increases the HOMO energy of a graphene sheet, and the nitrogen atom is not stable due to its 3-valent character. This raises an interesting research topic on the optimization of the N-substitution degree, and is important to many applications such as hydrogen storage and the tokamaks device. The electronic structure studies also explain well why nitrogen substitution increases the capacitance but decreases the electron conductivity of carbon electrodes as was experimentally observed in our experiments on the supercapacitor.

Introduction

Carbon materials such as carbon nanotubes and carbon nanofibers have been studied extensively for hydrogen storage. However, the experimentally obtained results are still controversial due to lack of reproducibility. In the absence of doped catalysts, a nondissociative physical adsorption mechanism was suggested to be a dominant mechanism for hydrogen storage.[1,2] Unfortunately, theoretical calculations showed that single wall carbon nanotubes (SWNTs) could store only 0.8 wt % of hydrogen at 133 K and 300 Torr if only the physisorption process dominates without the dissociation of H_2.[3]

Smalley suggested that hydrogen storage could be enhanced, if, in addition to molecular H_2 adsorption, atomic hydrogen was bonded to the walls of carbon nanotube.[4] The experimental study of Yang et al.[5] suggested that hydrogen molecules can dissociate over Ni and Mg catalysts followed by spillover to the walls of carbon nanotubes, but the reported hydrogen uptake was still lower than 1.0%. Alkali-doping was reported to be able to increase hydrogen uptake to more than 10%.[6] But it has been confirmed that the reported high hydrogen uptake was due to moisture adsorption.[7,8] Our recent ab initio study also confirmed that alkali-doping might not play any positive role in hydrogen storage in carbon materials at ambient conditions.[9]

Elemental substitution is another option to increase hydrogen atom bonding on carbon materials thus improving hydrogen uptake. There are several experimental efforts about the effect of nitrogen substitution on hydrogen storage. Bai et al.[10] reported that carbon nitride nanobells could adsorb up to 8 wt % of H_2 under ambient pressure and at a temperature of 300 °C. The hydrogen adsorption capacity reported by Badzian et al.[11] was much lower, ca. 0.7−0.8 wt % in carbon materials containing ca. 1% nitrogen at room temperature and 7 MPa. Once again, the hydrogen uptake result reported by Bai et al.,[10] which looks very promising, has not been confirmed yet. A theoretical study, which has not appeared, would be very useful for the determination of the reliability of the results reported by Bai et al.

In our recent experimental development of carbon electrode materials for the supercapacitor, we also found that nitrogen substitution in carbon materials can effectively improve the capacitance of the carbon electrode.[12,13] More recent results and the experimental details will be given in the Results and Discussion sections. But the corresponding mechanism is still left unclear.

This paper aims to theoretically investigate the interaction between hydrogen atoms and nitrogen-substituted carbon materials, and to clarify the role of nitrogen substitution in hydrogen adsorption. In addition to hydrogen storage, the achieved results will also be useful to several other areas such as semiconductor technology, astrophysics, and plasmas surface interactions in controlled fusion devices called tokamaks, in which hydrogen atom adsorption on carbon materials is an important issue. Meanwhile, the relevant electronic structure studies on nitrogen-substituted carbon materials will also provide useful information to other non-hydrogen related areas such as electron conductivity and capacitance as electrode materials in the supercapacitor.

Model and Methods

The Gaussian 98 package[14] was used to undertake the molecular orbital theory calculations. The detailed methodology for calculation using this package is described elsewhere.[15] B3LYP/3-21g(d,p) was used for geometry optimization and frequency calculation, and B3LYP/6-31g(d,p) for SCF energy calculations. The p functions are specifically added to hydrogen

* To whom all correspondences should be addressed. E-mail: johnz@cheque.uq.edu.au. Fax: 61-7-3365-6074.
† University of Queensland.
‡ National Institute of Advanced Industrial Science and Technology.
§ Curtin University of Technology.

10.1021/jp051787o CCC: $30.25
Published on Web 08/16/2005

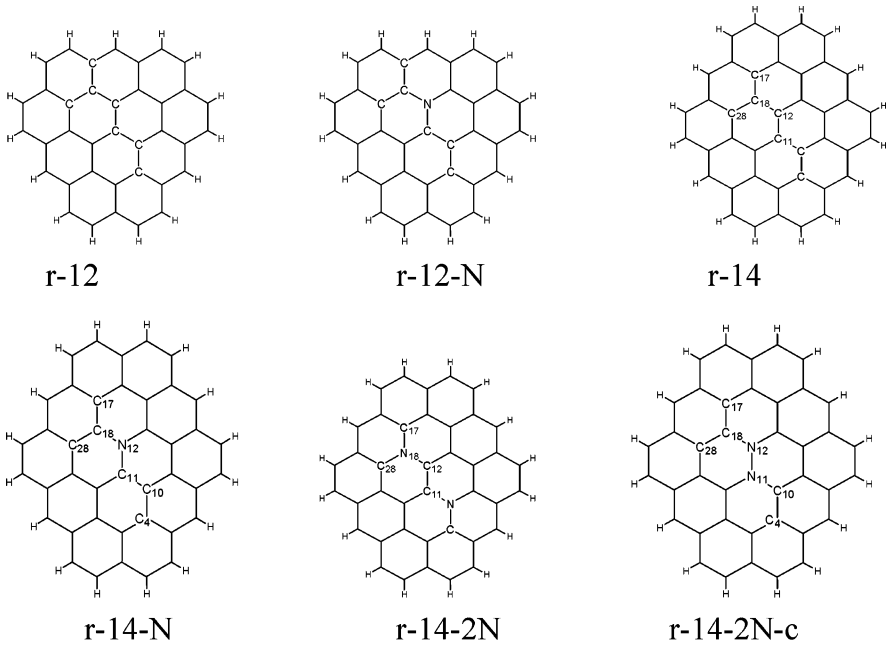

Figure 1. Graphite structure models to be used in this study.

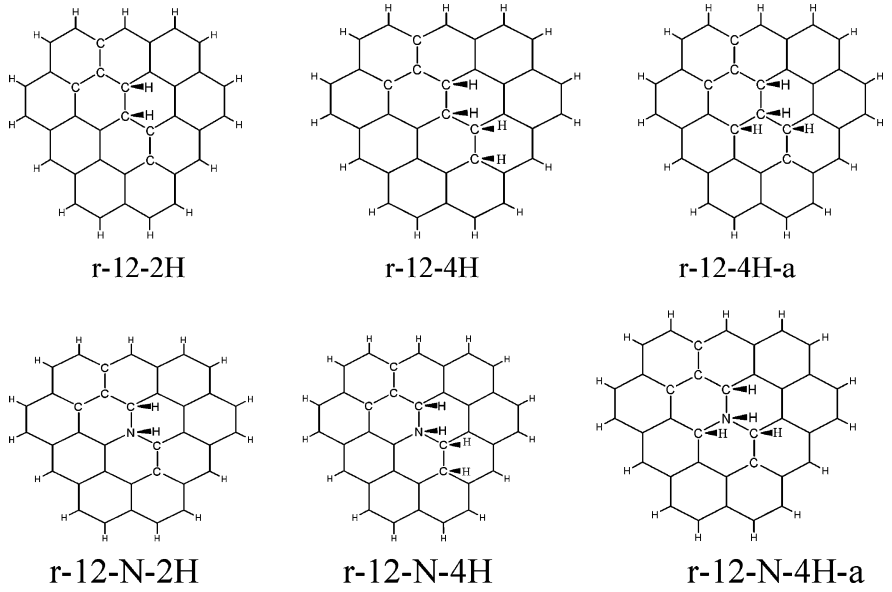

Figure 2. Hydrogen adsorption on models r-12 and r-12-N.

atoms in the basis set, thus 3-21g(d,p) and 6-31g(d,p) are used in the present calculations. Such a configuration can produce a good balance between calculation accuracy and computational time.[16] To further confirm the validity of this configuration, a higher level model chemistry B3LYP/6-31++g(d,p)//B3LYP/6-31g(d,p) will also be used to test some results. As carbon nanotubes are essentially rolled up graphite sheets, we use graphene sheets instead of the carbon nanotubes in our theoretical calculations. The large size of the carbon nanotubes causes difficulty with the computational time in the density functional theory study.

Full size optimization (instead of restricted optimization) was conducted throughout this paper. The heat of adsorption (ΔH) was determined as the difference between the total energy of the optimized system and the sum of the energies of the corresponding graphite model and gas molecules. The adsorption energy (ΔE) is negative ΔH. The higher the ΔE value, the stronger the adsorption is.

Results

The graphite structure models used in this study are illustrated in Figure 1. Models r-12 and r-14 contain 12 and 14 aromatic rings, respectively. Structure model r-12-N is obtained by replacing one carbon atom of model r-12 with one N atom; similarly, structure models r-14-N and r-14-2N are obtained by replacing one and two carbon atoms of model r-14 with one and two N atoms, respectively. Model r-14-2N-c means two substitutional nitrogens are next to each other.

We first calculated the adsorption of two or four hydrogen atoms on graphene structure models r-12 and r-12-N as shown in Figure 2 and the adsorption energies are shown in Table 1. One can see that for the same number of hydrogen atoms adsorbed on the same corresponding positions, the ΔE_H (adsorption energy per hydrogen atom) value on r-12-N is much lower than that on model r-12. For four hydrogen atoms adsorbed on both models r-12 and r-12-N, the adsorption energy is dependent on the distribution of the adsorbed hydrogen atoms: the line-

TABLE 1: Adsorption Energy of H Atoms on Models r-12 and r-12-N at B3LYP/6−31g(d,p)//B3LYP/3-21g(d,p)

model	ΔE_H (kJ/mol·H)	model	ΔE_H (kJ/mol·H)
r-12-2H	147	r-12-N-2H	83
r-12-4H	166	r-12-N-4H	137
r-12-4H-a	132	r-12-N-4H-a	93

distribution such as r-12-4H and r-12-N-4H has a higher adsorption energy than the cross-distribution such as r-12-4H-a and r-12-N-4H-a. This is an indication that it may be difficult for every carbon atom on the basal plane to adsorb one hydrogen atom. It is more possible that the adsorbed hydrogen atoms will be line-distributed leaving some carbon atoms vacant. The calculations by Bauschlicher[17] also showed that it is difficult to achieve 100% atomic H coverage on a (10,0) nanotube, and 50% coverage, which corresponds to about 4 wt % storage of H, is more favorable. On an extended $C_{200}H_{120}$ (10,0) tube, Bauschlicher[17] proposed different hydrogen distribution forms such as "single lines", "pairs of lines", "spiral", and "rings" for the 50% coverage.

It may not be sufficient to determine whether nitrogen substitution decreases hydrogen adsorption energy or not just based upon one size of graphene structure and one substitutional nitrogen. Next, we calculate a relatively larger structure with a different electron spin state and a different number of substitutional nitrogen atoms in order to confirm the above results. In details, model r-12 has an odd number of electrons with an open-shell electron structure, and it becomes a closed-shell structure by one substitutional nitrogen; while the structure model r-14 to be studied next has an even number of electrons with closed-shell structure, and it becomes an open-shell structure by one substitutional nitrogen and remains a closed-shell structure after incorporating two substitutional nitrogen atoms.

The adsorptions of 2 to 10 hydrogen atoms on models r-14, r-14-N, and r-14-2N are shown in Figure 3 and the corresponding adsorption energies are shown in Table 2 (columns 1 to 6). For more than two hydrogen atoms adsorbed on these three models, line-distributed adsorption is again found to be more thermodynamically favorable than cross-distributed adsorption. Therefore only line-distributed adsorptions are shown in Figure 3. The following observations can be made: (1) Similar to the adsorption on models r-12 and r-12-N, the adsorption energy on model r-14-N is also lower than that on model r-14 despite the change of the graphene size and electron spin state. (2) The hydrogen adsorption energies of models r-14-2H and r-14-4H are closer to that of models r-12-2H and r-12-4H, respectively, that is, for the same number of hydrogen atoms adsorbed on the same corresponding positions, the adsorption energies on models r-12 and r-14 are closer to each other. Similar observations can be made on models r-12-N and r-14-N. Such a consistency validates the selection of molecular structures in this study. (3) For hydrogen adsorption on model r-14-2N, the adsorption energy decreases gradually with the increase in the number of adsorbed hydrogen atoms, while on models r-14 and r-14-N, an opposite trend is observed. The reason may be that the conjugation of π electrons of models r-14 and r-14-N is strong, making it relatively difficult for the first two hydrogen atoms to be adsorbed. With the increase in the adsorbed hydrogen atoms, the conjugation of π electrons of models r-14 and r-14-N becomes weaker and the hydrogen adsorption energy becomes higher. On the other hand, two substitutional nitrogen atoms of model r-14-2N already weaken the conjugation of the π electrons due to the 3-valent character of N atoms, resulting in the higher adsorption energy of the first two hydrogen atoms (as model r-14-2N-2H). (4) With the increase in the adsorbed hydrogen atoms, the adsorption energies on models r-14, r-14-N, and r-14-2N become nearly constant. The hydrogen adsorption energies on models r-14-N and r-14-2N on the constant level are very close, both lower than that on model r-14. Now the contradiction arises. From observations (1) and (4), nitrogen substitution decreases the hydrogen adsorption energy. But observation (3) suggests that nitrogen substitution decreases the conjugation of π electrons thus should improve the hydrogen adsorption energy on N-substituted graphene.

To resolve the above controversy, we may clarify one question first, that is, why the hydrogen adsorption energy of model r-14-2N-2H is much higher than that of the other models in Figure 3. The key reason is that on model r-14-2N-2H, the two adsorbed hydrogen atoms are not on the top of any substitutional nitrogen atom but on the neighboring C-atoms. This indicates that substitutional nitrogen atoms increase the adsorption energy of hydrogen atoms on-top of the neighboring C-atoms. The nitrogen atoms are not stable sites for hydrogen adsorption due to its 3-valent character. So when more H atoms started to be adsorbed on the N atoms, such as models r-14-2N-4H and r-14-2N-6H, the hydrogen adsorption becomes lower until a constant level has been reached. This is confirmed by our further calculations on more H-atom adsorption on model r-14-2N with no H-atoms adsorbed on-top of the substitutional nitrogen atoms (see Figure 4 and column 8 of Table 2). One can see that the adsorption energies are rarely affected by the increase in the number of adsorbed hydrogen atoms if all the hydrogen atoms are adsorbed on the neighboring C-atoms instead of the nitrogen atoms. Further support information will be obtained from the discussion of the electronic structures.

We tested some adsorption energies using the higher level model chemistry B3LYP/6-31++g(d,p)//B3LYP/6-31g(d,p), and the results are the same as those from the lower level model chemistry (see Table 2).

For hydrogen adsorption on model r-14-2N-c, the N−N bond is broken after both substitutional nitrogens are attached with hydrogens. As a result, the substitutional nitrogens become edge sites (see Figure 5). This is beyond this study and r-14-2N-c will not be further addressed in the following discussion. As one substitutional nitrogen atom changes the electron spin state of a graphene structure, the next discussion on the change of electronic structures caused by nitrogen substitution will focus on the comparison of models r-14 and r-14-2N.

Discussion

The bond lengths and atom charges in the central part of structure models r-14 and r-14-2N are shown in Table 3. The C−C bond lengths in model r-14 are around 1.42 Å, in agreement with experimental data.[18] Elemental substitution changes the bond lengths. The N−C bonds of model r-14-2N are shorter than the C−C bonds of model r-14 at the corresponding positions. This means that nitrogen substitution stabilizes the graphene structure, which is consistent with the result reported by Türker and Gümüs.[19] This may also be the reason that nitrogen-substituted carbon has the mechanical property compared to diamond.[20] But such a stabilization is through the stronger in-plane C−N σ-bond not through the off-plane π bond. The π electrons become less conjugated by N-substitution (as mentioned above and will also be shown in more detail next). The charge distribution also becomes different after elemental substitution. C_{18} of model r-14 is positively charged. N_{18} of model r-14-2N is negatively charged probably due to the high electronegativity of N.

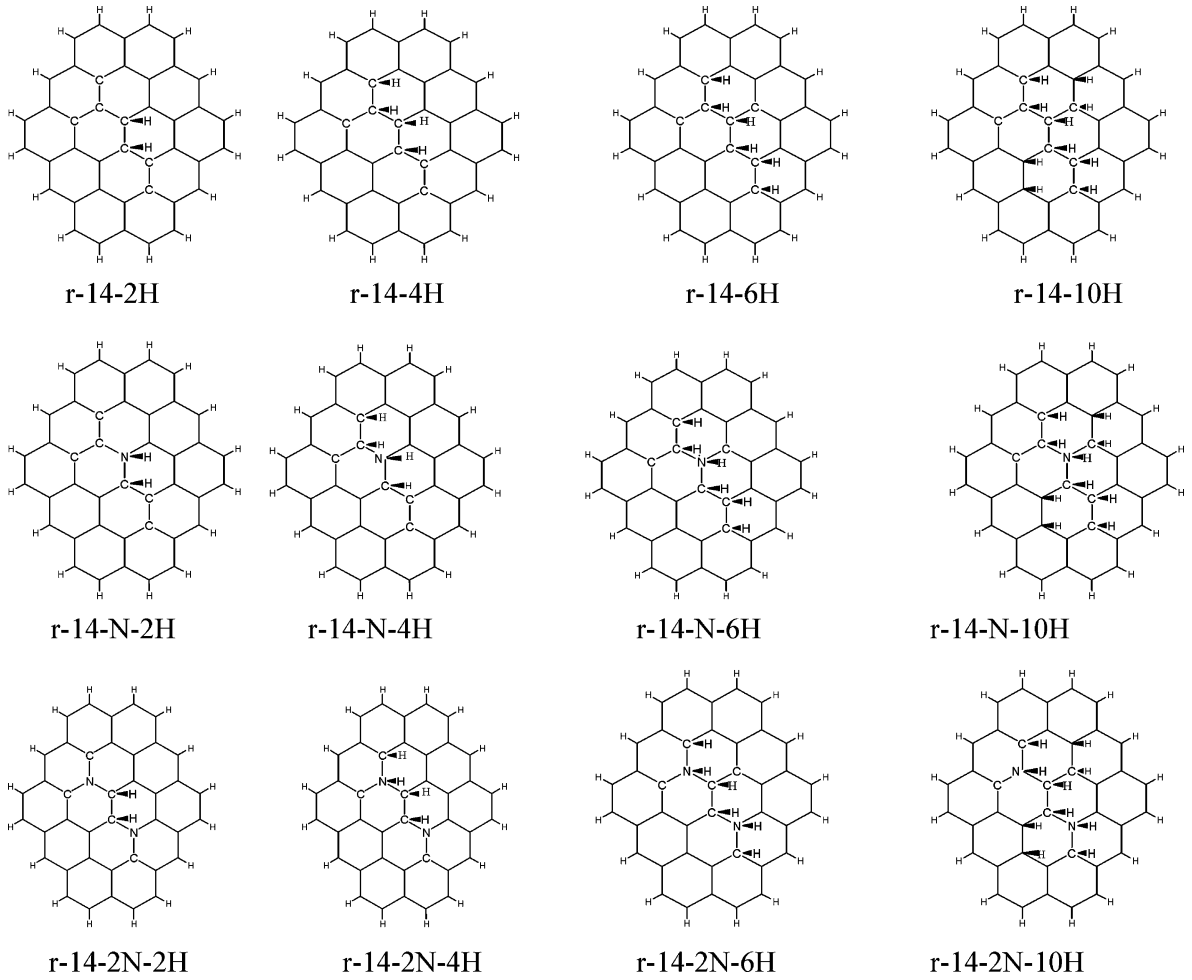

Figure 3. Hydrogen adsorption on graphene without and with one or two substitutional N atoms.

TABLE 2: Adsorption Energies of Hydrogen Atoms on Models r-14, r-14-N, and r-14-2N[a]

model	ΔE_H (kJ/mol·H)	model	ΔE_H (kJ/mol·H)	model	ΔE_H (kJ/mol·H)	model	ΔE_H (kJ/mol·H)
r-14-2H	151 (153)	r-14-N-2H	97	r-14-2N-2H	221 (224)	r-14-2N-2H-neighb	221 (224)
r-14-4H	167	r-14-N-4H	143	r-14-2N-4H	172 (175)	r-14-2N-4H-neighb	210 (212)
r-14-6H	180	r-14-N-6H	168	r-14-2N-6H	166 (168)	r-14-2N-6H-neighb	213 (216)
r-14-10H	176 (175)	r-14-N-10H	165	r-14-2N-10H	163 (165)	r-14-2N-10H-neighb	216 (218)

[a] Note: (1) model r-14-2N-2H is the same as r-14-2N-2H-neighb; (2) the energy data in parentheses are from B3LYP/6-31++g(d,p)//B3LYP/6-31g(d,p), the data outside the parentheses are from B3LYP/6-31g(d,p)//B3LYP/3-21g(d,p).

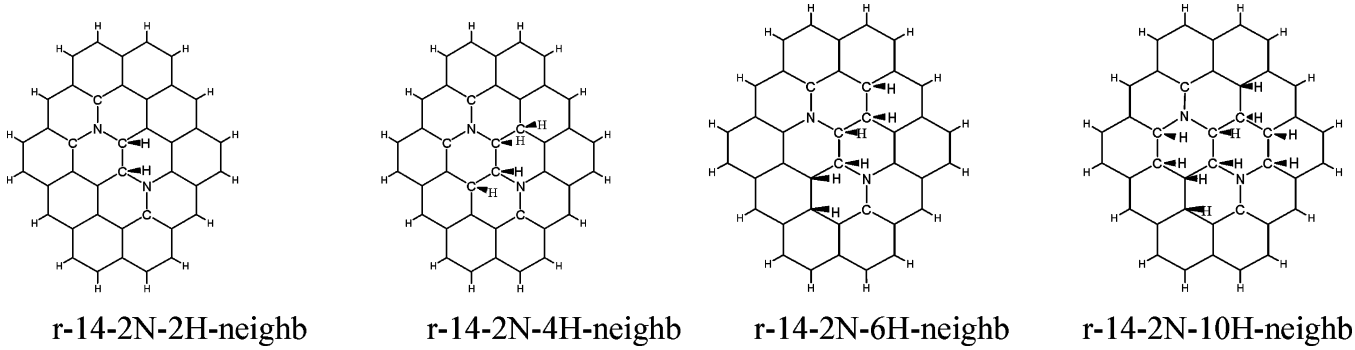

Figure 4. Hydrogen adsorption on the neighboring C-sites of the substitutional N atoms on model r-14-2N (note: r-14-2N-2H-neighb is the same as r-14-2N-2H).

The vibration bands originating from C−N bonds of model r-14-2N are at 1305 cm^{-1} (from B3LYP/6-31g(d,p)), and the experimentally obtained bands for aromatic C−N bonds vibration are between 1270 and 1340 cm^{-1}.[21] The consistency of our calculations with the experimental values confirms the validity of our calculation model chemistry including the selected model chemistry and molecular structures.

The energies of HOMOs (highest occupied molecular orbitals) and LUMOs (lowest unoccupied molecular orbitals) of models r-14 and r-14-2N are shown in Table 4 and the electron-wave

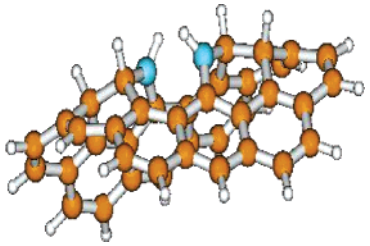

Figure 5. Adsorption of six hydrogen atoms on r-14-2N-c (the two blue atoms are nitrogen atoms).

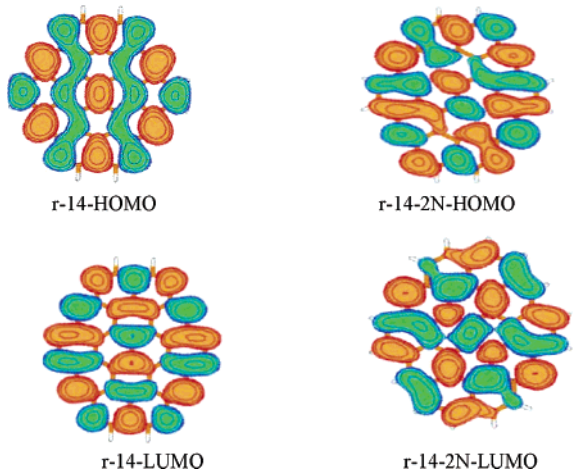

Figure 6. The electron-wave distributions of HOMOs and LUMOs of models r-14 and r-14-2N.

TABLE 3: Atomic Charges and Bond Lengths, Electrostatic Potentials of Models r-14 and r-14−2N (from B3LYP/6−31g(d,p)//B3LYP/3-21g(d, p))

bond lengths (Å)		atom charges[a]	
r-14	r-14-2N	r-14	r-14-2N
$C_{18}-C_{28}$: 1.419	$N_{18}-C_{28}$: 1.419	C_{12}: 0.089	C_{12}: +0.2875
$C_{18}-C_{12}$: 1.430	$N_{18}-C_{12}$: 1.388	C_{28}: −0.028	C_{28}: +0.2308
$C_{18}-C_{17}$: 1.422	$N_{18}-C_{17}$: 1.422	C_{18}: 0.079	N_{18}: −0.8675
$C_{11}-C_{12}$: 1.411		C_{17}: −0.030	C_{17}: +0.2493

[a] Based upon the sum of Mulliken charges = 0.

TABLE 4: Energies of HOMOs and LUMOs of Models r-14 and r-14-2N (hartrees)

r-14		r-14-2N		H
LUMO	HOMO	LUMO	HOMO	SOHO
−0.0826	−0.1753	−0.0832	−0.1146	−0.3162

distributions of the HOMO and LUMO are shown in Figure 6. HOMO is a π character orbital. Table 4 shows that N-substitution greatly increases the energy level of HOMO. As the energy of SOMO (single occupied molecular orbital) of hydrogen is closer to that of HOMO (rather than LUMO) of model r-14 or r-14-2N, hydrogen is adsorbed on the basal plane of the graphene through the interaction of SOMO of hydrogen with HOMO (instead of LUMO) of model r-14 or r-14-2N. The energy difference between the HOMO of model r-14-2N and the SOMO of hydrogen is bigger than that between the HOMO of model r-14 and the SOMO of hydrogen; this is why the adsorption energy of H atoms on N-substituted graphene is lower than that on pure graphene when hydrogen atoms are adsorbed on both substitutional N atoms and the neighboring C-atoms as shown in Figures 2 and 3.

One can see from Figure 6 that N-substitution not only changes the electron-wave distribution around the nitrogen atom but also causes the redistribution of π electron density along the whole graphene structure layer. A comparison of the HOMOs of r-14 and r-14-2N clearly shows that the π electrons of the latter are less conjugated than that of the former. This supports our previous conclusion that substitutional nitrogen atoms improve the adsorption energy of hydrogen atoms on-top of the neighboring C-atoms. For the case of a smaller number of N atoms among many C atoms, the probability of H-adsorption on-top of C atoms is apparently higher. So the adsorption patterns with H on-top of C with N remaining free could be expected to prevail. For an optimal degree of N-substitution, the H adsorption could thus be increased. To optimize the degree of N-substitution in carbon materials is thus a promising area.

TABLE 5: Specific Capacitances Per Unit Surface Area (SC) in 1 M H_2SO_4 and Specific Resistivities (Re) of Carbon Electrodes in Dry Condition

sample[a]	*N*[b] (wt %)	SC[c] (F/m^2)	Re[d] (Ω cm)
MFCAG-1273	14.66	0.29	11.3
RFCAG-1273	0	0.15	2.16

[a] Samples: MFCAG-1273 and RFCAG-1273 were synthesized from melamine-formaldehyde and resorcinol-formaldehyde resins, respectively, and carbonized at 1273 K in an inert atmosphere. [b] *N*: nitrogen content (wt %) by elemental analysis. [c] SC: specific capacitance per unit surface area (F/cm^2) measured by cyclic voltammograms in 1 M H_2SO_4 with a sweep rate of 1 mV/s. [d] Re: specific resistivity (Ω cm) measured by the four probe method.

Our recent results on the corresponding capacitance and specific resistivity of nitrogen-enriched carbon aerogels in a supercapacitor are shown in Table 5. The experimental details are reported in refs 13 and 22. One can see that the nitrogen-enriched carbons have a larger specific capacitance per unit surface area, and a bigger specific electrical resistivity compared with the carbons without nitrogen. This can also be explained by our electronic study.

The less conjugated π electrons of N-substituted carbon can lower the electron conductivity of nitrogen-substituted carbon materials (or increase the electrical resistivity). The higher energy of HOMO of model r-14-2N compared with model r-14 means that N-substituted carbon can be more positively charged when used as anode materials in the supercapacitor (the more positively charged carbon surface can adsorb more negative charges), thus having larger capacitance.

As nitrogen substitution increases the capacitance but also decreases the electron conductivity of the carbon electrode, it is important to develop the nitrogen-substituted carbon electrodes with the best configuration of capacitance and conductivity. Once again, to obtain the optimal nitrogen content and distribution is also a promising direction in electrode materials research. Certainly, computational chemistry is a powerful tool and will play a key role in our future optimization research.

Conclusions

Nitrogen substitution stabilizes the structure, weakens the π electron conjugation, and increases the HOMO energy of a graphene sheet. N atoms are not stable sites for hydrogen adsorption due to its 3-valent structure. Consequently, nitrogen substitution decreases the hydrogen adsorption energy if hydrogen atoms are adsorbed on both nitrogen atoms and the neighboring carbon atoms. On the contrary, the hydrogen adsorption energy can be increased if hydrogen atoms are adsorbed only on the neighboring carbon atoms. The less conjugated π electrons explain the lower electron conductivity and the higher HOMOs energy accounts for the improved capacitance after nitrogen substitution.

Acknowledgment. Financial support for this project from the Australian Research Council Discovery Grant (APD for Z.H.Z.) is gratefully acknowledged.

References and Notes

(1) Dillon, A. C.; Jones, K. M.; Bekkedahl, T. A.; Kiang, C. H.; Bethune, D. S.; Heben, M. J. *Nature* **1997**, *385*, 377.

(2) Ye, Y.; Ahn, C. C.; Witham, C.; Fultz, B.; Liu J.; Rinzler, A. G.; Collbert, D.; Smith, K. A.; Smalley, R. E. *Appl. Phys. Lett*. **1999**, *74*, 2307.

(3) Wang, Q.; Johnson, J. K. *J. Chem. Phys*. **1999**, *110*, 577.

(4) Bauschlicher, C. W., Jr. *Nano Lett.* **2001**, *1*, 223.

(5) Lueking, A.; Yang, R. *J. Catal*. **2002**, *206*, 165−168.

(6) Chen, P.; Wu, X.; Lin, J.; Tan, K. L. *Science* **1999**, *285*, 91.

(7) Yang, R. T. *Carbon* **2000**, *38*, 623.

(8) Pinkerton, F. E.; Wicke, B. G.; Olk, C. H.; Tibbetts, G. G.; Meisner, G. P.; Meyer, M. S.; Herbst, J. F. *J. Phys. Chem. B* **2000**, *104*, 9460.

(9) Zhu, Z. H.; Lu, G. Q.; Seam, S. *Carbon* **2004**, *42*, 2509.

(10) Bai, X. D.; Zhong, D. Y.; Zhang, G. Y.; Ma, X. C.; Liu, S.; Wang, E. G.; Chen, Y.; Shaw, D. T. *Appl. Phys. Lett*. **2001**, *79*, 1552.

(11) Badzian A.; Badzian, T.; Breval, E.; et al. *Thin Solid Films* **2001**, *398*, 170.

(12) Kodama, M.; Yamashita, J.; Soneda, Y.; Hatori, H.; Nishimura, S.; Kamegawa, K. *Mater. Sci. Eng., B* **2004**, *108*, 156.

(13) Hulicova, D.; Kodama, M.; Yamashita, J.; Soneda, Y.; Hatori, H. *Chem. Mater*. Accepted for publication.

(14) Frisch, M. J.; Trucks, G. W.; Schlegel, H. B.; Scuseria, G. E.; Robb, M. A.; Cheeseman, J. R.; et al. *Gaussian 98*, Revision A.7; Gaussian, Inc.: Pittsburgh, PA, 1998.

(15) Foresman, J. B.; Frisch, A. *Exploring Chemistry with Electronic Structure Methods*, 2nd ed.; Gaussian: Pittsburgh, PA, 1996.

(16) Zhu, Z. H.; Lu, G. Q.; Yang, R. T.; Wilson, M. A. *Energy Fuels* **2002**, *16*, 847.

(17) Bauschlicher, C. W. *Nano Lett*. **2001**, *1*, 223.

(18) *Handbook of Chemistry and Physics*, 67th ed.; CRC Press: Cleveland, OH, 1978; p F158.

(19) Türker, L.; Gümüs, S. *J. Mol. Struct.* (*THEOCHEM*) **2004**, *679*, 143.

(20) Liu, A. Y.; Cohen, M. L. *Science* **1989**, *245*, 841.

(21) Gillan, E. G. *Chem Mater*. **2000**, *12*, 3906.

(22) Matsuoka, T.; Hatori, H.; Yamashita, J.; Kodama, M.; Miyajima, N. *Carbon* **2004**, *42*, 2346.